

Accurate quasinormal modes of the analogue black holes

Jerzy Matyjasek,^{1,*} Kristian Benda,^{1,†} and Maja Stafińska^{1,‡}

¹*Institute of Physics, Maria Curie-Skłodowska University*

pl. Marii Curie-Skłodowskiej 1, 20-031 Lublin, Poland

We study the quasinormal modes of the spherically-symmetric $(2 + 1)$ -dimensional analogue black hole, modeled by the “draining bathtub” fluid flow, and the $(3 + 1)$ -dimensional canonical acoustic black hole. In the both cases the emphasis is on the accuracy. Formally, the radial equation describing perturbations of the $(2 + 1)$ -dimensional black hole is a special case of the general master equation of the 5-dimensional Tangherlini black hole. Similarly, the $(3 + 1)$ -dimensional equation can be obtained from the master equation of the 7-dimensional Tangherlini black hole. For the $(2 + 1)$ -dimensional analogue black hole we used three major techniques: the higher-order WKB method with the Padé summation, the Hill-determinant method and the continued fraction method, the latter two with the convergence acceleration. In the $(3 + 1)$ -dimensional case, we propose the simpler recurrence relations and explicitly demonstrate that both recurrences, i.e., the eight-term and the six-term recurrences yield identical results. Since the application of the continued-fraction method require five (or three) consecutive Gauss eliminations, we decided not to use this technique in the $(3 + 1)$ -dimensional case. Instead, we used the Hill-determinant method in the two incarnations and the higher-order WKB. We accept the results of our calculations if at least two (algorithmically) independent methods give the same answer to some prescribed accuracy. Our results correct and extend the results existing in the literature and we believe that we approached assumed accuracy of 9 decimal places. In most cases, there is perfect agreement between all the methods; however, in a few cases, the performance of the higher-order WKB method is slightly worse.

I. INTRODUCTION

With the first detection of the gravitational waves, our hopes for opening of a new observational window increased significantly. And although currently we can only draw very general conclusions from the received signals, it is conceivable that the planned new generations of more sensitive detectors will provide us with detailed information regarding the nature of the astrophysical sources of the gravitational waves and the gravitational waves themselves. However, it is also conceivable

* jurek@kft.umcs.lublin.pl, jirinek@gmail.com

† kriben@gmail.com

‡ majastafinska@gmail.com

that extraction of the imprints of some concrete physical phenomena from the received signals may prove challenging. Therefore, while waiting for a significant breakthrough in the observational techniques and the next generations of the gravitational wave detectors, we should also focus on the experiments that can be, in principle, carried out in the laboratory. As the most common sources of detectable gravitational waves are black holes, it is natural that we should try to devise experimental setups for configurations that mimic astrophysical black holes.

Black holes are important components of many of our modern theories. Indeed, they play a crucial role in explaining the formation of galaxies, the creation and dynamics of accretion disks, active galactic nuclei, and gamma-ray bursts, to name just a few examples. They may also lead to some observable optical phenomena and (probably practically undetectable) Hawking radiation. Since Unruh's seminal paper on black hole evaporation in a laboratory [1], there has been a flurry of research on the so called analogue black holes and the interested reader is referred to the excellent review [2], research papers (see for example Refs. [3, 4]) and the numerous references cited therein. In this article we shall concentrate on the two models of the analogue black holes: (2+1)-dimensional acoustic black hole (also called the draining bathtub model) and (3+1)-dimensional canonical acoustic black hole [5]. Our task will be to determine complex frequencies of the quasinormal modes of such configurations.

Quasinormal modes are radiated in response to a weak disturbance or when the initial strong disturbance becomes weak. In all these cases, all information regarding the nature of the initial disturbances is washed out, and the black hole radiates its own characteristic frequencies [6–9]. Although both types of the analogue black holes have been considered earlier [10, 11], our objective is to extend the analysis of the quasinormal oscillations to higher fundamental modes and their overtones and to deliver highly accurate results that refine or correct the existing results in the literature. To accomplish this, depending on the specific mode, we have employed several methods, such as higher-order WKB with Padé summation¹, the Hill determinant method with convergence acceleration, and, additionally, in the case of the (2+1)-dimensional acoustic black hole, the continued fraction method also with convergence acceleration. Moreover, in the case of the canonical acoustic black hole, the Hill determinant method was used with two different recurrence relations. Since we have restricted ourselves to the three aforementioned methods, some promising approaches, such as the asymptotic iteration method [14] or the spectral method [15], were not employed.

¹ The analytic form of the WKB terms is known up to the 16th order (see Refs. [12, 13]). By higher-order WKB, we mean numerically calculated terms of at least the 50th-order.

Besides the fundamental modes, we have also determined a certain number of overtones (labeled by the overtone number $n \geq 1$), not only to capture the trend of the quasinormal frequency changes as n increases, but also because their calculation serves as the unique stress test for the adapted methods and algorithms. We accept the result of our calculations if at least two independent methods give the same answer to 9 decimal places, and if the results calculated using other competing methods considered in this paper differ from them only slightly. In doing so we have two goals in mind. First, the signal from the laboratory acoustic black holes will be contaminated and to extract the quasinormal frequency it is desirable to have at one's disposal the highly accurate theoretical predictions. Secondly, by demanding accuracy, one can compare the actual performance of various methods, analyze their strengths and weaknesses, and identify possible bottlenecks. The latter observation may be crucial in the case of 'difficult' potentials, where methods relying on the higher-order WKB-*Padé* approximation (and its variants) are especially valuable due to their universality and simplicity.

The paper is organized as follows. In Sec. II we briefly review the most important for our calculations features of the $(2+1)$ and $(3+1)$ -dimensional acoustic black holes and introduce the radial equations describing perturbations. In Sec. III the relation between the master equation of the D -dimensional Schwarzschild-Tangherlini and radial equations of the $(2+1)$ -dimensional and $(3+1)$ -dimensional acoustic black holes is investigated. In the case of the $(3+1)$ -dimensional acoustic black hole, we also propose a slightly more complex series solution to the radial equation, which, nevertheless, yields a simpler six-term recurrence. (The coefficient of the recurrence relations for the D -dimensional black hole are relegated to the appendix). In Secs. IV and V we describe our ideas and strategies for calculating the complex frequencies of the quasinormal modes of the acoustic black holes. In Sec. VI, we present the results of our high-accuracy calculations and compare them with the ones previously published. The final discussion and conclusions are given in Sec. VII. Throughout the paper, we shall follow the terminology used in the black hole physics.

II. $(2+1)$ -DIMENSIONAL AND $(3+1)$ -DIMENSIONAL ACOUSTIC BLACK HOLES

A. $(2+1)$ -dimensional black holes

The line element of the static $(2+1)$ -dimensional acoustic black hole (also called the draining bathtub model) can be written in the form [5, 10]

$$ds^2 = - \left(c_s^2 - \frac{A^2}{r^2} \right) dt^2 + \frac{2A}{r} dt dr + dr^2 + r^2 d\phi^2, \quad (1)$$

where A is a positive constant related to the radial velocity of the background fluid

$$v = -\frac{A}{r} \quad (2)$$

and c_s is the speed of sound. It describes $(2 + 1)$ -dimensional flow with a sink at the origin. The fluid is locally irrotational, (i.e., vorticity free), barotropic and inviscid. The acoustic event horizon is located at $r_H = A/c_s$.

The propagation of sound waves in the acoustic geometry is described by a massless minimally coupled scalar field equation

$$g^{ab}\nabla_a\nabla_b F = 0, \quad (3)$$

which, for the line element (1), can be separated using simple substitution

$$F(t, r, \phi) = \psi(r)e^{i(m\phi - \omega t)}. \quad (4)$$

Now, rescaling the radial coordinate and the frequency according to $r \rightarrow rc_s/A$ and $\omega \rightarrow \omega c_s^2/A$, after some manipulations [5, 10], one obtains

$$\frac{d^2}{dr_\star^2}\psi + (\omega^2 - V(r))\psi = 0, \quad (5)$$

where

$$V(r) = \left(1 - \frac{1}{r^2}\right) \left[\frac{1}{r^2} \left(m^2 - \frac{1}{4}\right) + \frac{5}{4r^4} \right], \quad (6)$$

r_\star is the standard tortoise radial coordinate, m is the azimuthal number, and $r_H = 1$.

B. (3+1)-dimensional black holes

The line element describing the static $(3 + 1)$ -dimensional nonrotating acoustic black hole [5] has the following form (for the discussion and explanations see e.g., Ref. [10])

$$ds^2 = -c_s^2 \left(1 - \frac{r_0^4}{r^4}\right) dt^2 + \left(1 - \frac{r_0^4}{r^4}\right)^{-1} dr^2 + r^2 (d\theta^2 + \sin^2\theta d\phi^2), \quad (7)$$

where c_s is the speed of sound and r_0 is the normalization constant. It is the acoustic metric related to the spherically-symmetric flow of incompressible barotropic fluid. The time-dependent version of this metric may be constructed around spherically-symmetric bubble with oscillating radius (see [5] and the references therein).

The propagation of small disturbances is described by the minimally coupled massless Klein-Gordon equation, which, because of the symmetries, can easily be separated using

$$\psi(t, r, \theta, \phi) = \frac{\psi(r)}{r} e^{-i\omega t} Y_{sm}(\theta, \psi), \quad (8)$$

where Y_{sm} are the spherical harmonics (s is the multipole number). When presenting and comparing our numerical results, we shall use units in which $r_0 = 1$ and $c_s = 1$. This can be achieved with the substitution $r \rightarrow r_0 r$ and $\omega \rightarrow \omega c_s$. Consequently, the radial equation assumes the general form (5) with

$$V(r) = \left(1 - \frac{1}{r^4}\right) \left(\frac{s(s+1)}{r^2} + \frac{4}{r^6}\right). \quad (9)$$

III. D -DIMENSIONAL SCHWARZSCHILD-TANGHERLINI BLACK HOLES VS. ACOUSTIC BLACK HOLES

We start our discussion of the acoustic black holes with the observation that the radial equations of the (2+1) and (3+1)-dimensional black holes are formally similar to the analogous equations of ($D = 5$)-dimensional and ($D = 7$)-dimensional Schwarzschild-Tangherlini black holes, respectively. More precisely, the radial equations describing perturbations of the acoustic black holes can be obtained from the master equation of the D -dimensional Schwarzschild-Tangherlini black hole by the appropriate choice of parameters. Therefore, before addressing the particular case of hydrodynamic black holes, let us briefly discuss the properties of the D -dimensional solution that are important from our perspective.

A. Master equation.

The D -dimensional generalization of the Schwarzschild black hole is described by the line element

$$ds^2 = -f(r)dr^2 dt^2 + \frac{dr^2}{f(r)} + r^2 d\Omega_{D-2}^2 \quad (10)$$

where

$$f(r) = 1 - \frac{\mathcal{M}}{r^{3-D}} \quad (11)$$

and $d\Omega_{D-2}^2$ is a metric on a unit ($D - 2$)-dimensional sphere. The black hole mass M is related to the parameter \mathcal{M} by a simple relation

$$M = \frac{(D-2)\omega_{D-2}\mathcal{M}}{16\pi G_D} \quad (12)$$

with

$$\omega_{D-2} = \frac{2\pi^{(D-2)/2}}{\Gamma[(D-1)/2]}. \quad (13)$$

In what follows, we shall use the geometric units and express our numerical results assuming $\mathcal{M} = 1$.

Now, the differential (master) equation describing the massless scalar, gravitational tensor, gravitational vector, electromagnetic vector, and electromagnetic scalar perturbations of the D -dimensional Schwarzschild-Tangherlini black hole ($D > 4$) can be written in a compact form [16–18]:

$$\frac{d^2}{dr_*^2}\psi + \left\{ \omega^2 - f(r) \left[\frac{l(l+D-3)}{r^2} + \frac{(D-2)(D-4)}{4r^2} + \frac{(1-j^2)(D-2)^2}{4r^{D-1}} \right] \right\} \psi = 0, \quad (14)$$

where j is given by

$$j = \begin{cases} 0, & \text{massless scalar and gravitational tensor perturbations.} \\ 2, & \text{gravitational vector perturbations,} \\ \frac{2}{D-2}, & \text{electromagnetic vector perturbations} \\ 2 - \frac{2}{D-2}, & \text{electromagnetic scalar perturbations.} \end{cases} \quad (15)$$

Of course, from a general point of view, we are not confined to the values of the parameter j listed in Eq. (15). By doing so, we can gain a new interpretation of Eq. (14) at the expense of losing its original interpretation. We will make use of this fact later in this work.

The quasinormal modes are defined as the solutions of the master equation that are purely ingoing as $r_* \rightarrow -\infty$ and purely outgoing as $r_* \rightarrow \infty$ with the asymptotic behaviors $e^{-i\omega r_*}$ and $e^{i\omega r_*}$, respectively. Now, the standard procedure is to construct a series expansion of the perturbation ψ with the required asymptotics. The first choice that has been adopted in this paper is to take

$$\psi(r) = \left(\frac{r-1}{r} \right)^{-i\omega/(D-3)} e^{i\omega r} \sum_{k=0}^{\infty} a_k \left(\frac{r-1}{r} \right)^k, \quad (16)$$

for the even-dimensional case and

$$\psi(r) = \left(\frac{r-1}{r+1} \right)^{-i\omega/(D-3)} e^{i\omega r} \sum_{k=0}^{\infty} a_k \left(\frac{r-1}{r} \right)^k. \quad (17)$$

for the odd-dimensional case. The even-dimensional expansion is given here for completeness. Upon the substitution of (16) and (17) into the master equation one obtains the recurrence relations for the expansion coefficients a_k . As a result, we will obtain $(2D-5)$ -term recurrence relation for the even-dimensional black hole and $(2D-6)$ -term recurrence for the odd-dimensional black hole.

It should be noted that, depending on a specific dimension, the functions (16) and (17) can be modified to yield even simpler recurrences. Indeed, for the (3 + 1)-analogue black hole, the expansion

$$\psi(r) = \left(\frac{r-1}{r+1}\right)^{-i\omega/4} e^{i\omega r} e^{-i\omega \arctan(r)/2} \sum_{k=0}^{\infty} a_k \left(\frac{r-1}{r}\right)^k \quad (18)$$

leads to the six-term recurrence. It is an improvement over the method based on the expansion (17). All the calculations presented in this paper regarding the (3 + 1)-dimensional hydrodynamic black hole have been carried out using both expansions, leading to the results that are in perfect agreement with each other.

B. The recurrence relations for the (2 + 1)-dimensional acoustic black hole

The radial equation of the (2 + 1)-dimensional acoustic black hole is formally identical to the analogous equation describing the electromagnetic vector perturbations of the five-dimensional Schwarzschild -Tangherlini black hole. Indeed, putting $D = 5$, $j = 2/3$, and $l = m - 1$ for $m \geq 1$, the master equation (14) reduces to Eq. (5) with the potential term given by (6), and one can use (A.1) and (A.2) to obtain the four-term recurrence relation

$$\alpha_k a_{k+1} + \beta_k a_k + \gamma_k a_{k-1} + \delta_k a_{k-2} = 0, \quad (19)$$

where

$$\begin{aligned} \alpha_k &= -8(1+k)(1+k-2\rho), \\ \beta_k &= 20k^2 + 4m^2 + 4k(5-16\rho) + 4(1-4\rho)^2, \\ \gamma_k &= 6 - 16k^2 + 32k\rho, \\ \delta_k &= -3 - 4k + 4k^2. \end{aligned} \quad (20)$$

Here $a_{-2} = a_{-1} = 0$, and (following tradition) we introduced $\rho = i\omega/2$. Of course, one can start with Eqs. (5) and (6) and construct the solution directly, identifying the singular points of the differential equations. Then, it suffices to substitute expansion (17) into the equation (5) and use the standard techniques to construct the coefficients of the recurrence relation.

C. The recurrence relations for the (3+1)-dimensional acoustic black hole

A simple analysis shows that, formally, the radial equation of the (3 + 1)-dimensional acoustic black hole is a special case of the D -dimensional master equation with $D = 7$, $j = 3/5$ and

$l = (2s - 3)/2$. Unlike the previous case, however, this type of perturbation is not listed in Eq. (15), and the multipole number l is fractional. Now, to construct the recurrences, it suffices to make use of either (A.3) or (A.4). Alternatively, one may start with the potential (9) from the very beginning.

1. The eight-term recurrence relations

Inserting the series expansion (17) into the master equation one obtains the eight-term recurrence relations

$$a_{k+1} \alpha_k + a_k \beta_k + a_{k-1} \gamma_k + a_{k-2} \delta_k + a_{k-3} \kappa_k + a_{k-4} \lambda_k + a_{k-5} \mu_k + a_{k-6} \nu_k = 0, \quad (21)$$

with

$$a_{-6} = a_{-5} = a_{-4} = a_{-3} = a_{-2} = a_{-1} = 0, \quad (22)$$

where

$$\begin{aligned} \alpha_k &= -8(k+1)(k-\rho+1), \\ \beta_k &= 2(18k^2 + k(14 - 32\rho) + 14\rho^2 - 14\rho + s(s+1) + 4), \\ \gamma_k &= -2(36k^2 - 2k(34\rho + 9) + 33\rho^2 + 16\rho + s(s+1) + 2), \\ \delta_k &= 84k^2 - 152k(\rho+1) + 69\rho^2 + 142\rho + s(s+1) + 52, \\ \kappa_k &= -2(31k^2 - k(49\rho + 97) + 18\rho^2 + 80\rho + 60), \\ \lambda_k &= 29k^2 - 3k(12\rho + 43) + 9\rho^2 + 84\rho + 116, \\ \mu_k &= -8k^2 + k(6\rho + 46) - 18(\rho + 3), \\ \nu_k &= k^2 - 7k + 10. \end{aligned} \quad (23)$$

2. A different choice of the radial function $\psi(r)$

Now, let us consider a slightly modified radial function $\psi(r)$ defined as

$$\psi(r) = \left(\frac{r-1}{r+1}\right)^{-i\omega/4} e^{i\omega r} e^{-i\omega \arctan(r)/2} \sum_{k=0}^{\infty} a_k \left(\frac{r-1}{r}\right)^k. \quad (24)$$

It can be shown that such a choice leads to the six-term recurrence

$$a_{k+1} \alpha_k + a_k \beta_k + a_{k-1} \gamma_k + a_{k-2} \delta_k + a_{k-3} \kappa_k + a_{k-4} \lambda_k = 0, \quad (25)$$

with $a_{-4} = a_{-3} = a_{-2} = a_{-1} = 0$, where

$$\begin{aligned}
\alpha_k &= -4(k+1)(k-\rho+1), \\
\beta_k &= 4 + 14k^2 + s(s+1) + 2k(7-12\rho) + 12\rho(\rho-1), \\
\gamma_k &= -20k^2 + 28k\rho - 8\rho^2 + 4, \\
\delta_k &= 15k^2 - k(16\rho+15) + 4\rho^2 + 8\rho - 6, \\
\kappa_k &= -6k^2 + 4k(\rho+3) - 4\rho + 2, \\
\lambda_k &= (k-3)k.
\end{aligned} \tag{26}$$

In what follows, we shall use both recurrence relations.

IV. THE METHODS BASED ON THE RECURRENCE RELATIONS

A. The Hill determinant method

The recursion coefficients determined in the previous section can be utilized in either the Hill determinant method or the continued fraction method. In the context of the quasinormal modes of the black holes, the Hill determinant method has been used for the first time by Majumdar and Panchapakesan in Ref. [19]. For years it has been treated as a lesser relative to its more prominent cousins, as for example the Leaver method. The Hill determinant method has been criticized for rapid deterioration of the accuracy of the complex frequencies of the quasinormal modes, especially for the overtones, and the lack of a natural estimator of the error caused by a finite dimension of the Hill matrices. While some of the critique may be justified, it does not mean that the method should be abandoned. Even in its simplest version, the approximate results may be used as initial values for more sophisticated methods. Further improvements may lead to a substantial increase of its accuracy, which, with some additional effort, can be better than the accuracy of the Leaver method in its original form. The Hill determinant method is one of the three methods used in this paper. Here we will present only its main features.

We start with the four-term recurrence. The condition that the nontrivial solutions of the recurrence relation (19) exist is given by

$$\det \mathcal{H} = 0, \tag{27}$$

the complex plane some subset of the solutions with negative imaginary part of the frequency, which are identified as the quasinormal modes [19].

In a modified approach [20], we calculate solutions of the determinant equation order by order for increasing k up to some N and look for stable roots. The stable roots that approximate the exact quasinormal frequency migrate on the complex plane but they remain in the basin of convergence. We consider the roots as stable if for increasing k their location does not change to the assumed precision. Unfortunately, in many cases, such as when calculating higher overtones or when greater precision of the results is required, the convergence of the approximants may be slow. In this case one can increase N and accelerate convergence of the approximants using some standard techniques, as for example, the Padé summation or the Wynn algorithm.

The $(3 + 1)$ hydrodynamic black hole can be treated similarly. First, we construct the banded $(k \times k)$ matrices ($k = k_0, \dots, N$) of width eight (or six) and calculate their determinants. Subsequently we solve the resulting equations and search for stable roots. Finally, we accelerate convergence of the approximants ω_k . Since the construction of the tridiagonal matrices requires the execution of 5 (or 3) consecutive Gaussian eliminations, we will not employ this approach here.

B. The continued fractions method

The method of continued fractions is widely used in the context of the quasinormal modes. It is based on the profound relationship between the continued fractions and the three-term recursions. Here we give only a few basic facts that will be needed in our discussion.

Let us consider a four-term recurrence of the type (19). Generalizations to more complicated cases are obvious. Suppose that it has been transformed to a three-term recurrence

$$\alpha'_k a_{k+1} + \beta'_k a_k + \gamma'_k a_{k-1} = 0 \quad (32)$$

(with $a_{-1} = 0$) by the appropriate Gauss elimination. The primed coefficients are given by

$$\alpha'_k = \alpha_k, \quad (33)$$

$$\beta'_k = \begin{cases} \beta_k, & \text{for } k = 0, 1 \\ \beta_k - \delta_k \alpha'_{k-1} / \gamma'_{k-1} & \text{for } k \geq 2 \end{cases} \quad (34)$$

and

$$\gamma'_k = \begin{cases} \gamma_k, & \text{for } k = 0, 1 \\ \gamma_k - \delta_k \beta'_{k-1} / \gamma'_{k-1} & \text{for } k \geq 2. \end{cases} \quad (35)$$

As is well-known, the convergence condition for the series expansion (which is simultaneously the condition for the quasinormal modes) can be expressed in the form of an infinite continued fraction:

$$\beta'_0 - \frac{\alpha'_0 \gamma'_1}{\beta'_1 - \frac{\alpha'_1 \gamma'_2}{\beta'_2 - \frac{\alpha'_2 \gamma'_3}{\beta'_3 - \dots}}} = 0 \quad (36)$$

or, equivalently, in the more popular notation,

$$\beta'_0 - \frac{\alpha'_0 \gamma'_1}{\beta'_1 -} \frac{\alpha'_1 \gamma'_2}{\beta'_2 -} \frac{\alpha'_2 \gamma'_3}{\beta'_3 -} \dots = 0. \quad (37)$$

Inverting Eq. (36) n times, one obtains

$$\beta'_n - \frac{\alpha'_{n-1} \gamma'_n}{\beta'_{n-1} -} \frac{\alpha'_{n-2} \gamma'_{n-1}}{\beta'_{n-2} -} \dots - \frac{\alpha'_0 \gamma'_1}{\beta'_0} = \frac{\alpha'_n \gamma'_{n+1}}{\beta'_{n+1} -} \frac{\alpha'_{n+1} \gamma'_{n+2}}{\beta'_{n+2} -} \frac{\alpha'_{n+2} \gamma'_{n+3}}{\beta'_{n+3} -} \dots \quad (38)$$

If the recurrence is constructed for the radial equation (5), its minimal solutions correspond to the quasinormal modes. Now, our strategy is as follows: First, we (numerically) solve Eq. (36) truncated at some index N and identify the (approximate) quasinormal frequencies using some low-cost method. Subsequently, we increase N and analyze the migration of the quasinormal modes on the complex plane. In doing so, we obtain a series $\omega(N)$ that may or may not converge rapidly to the limiting value. In the latter case, we accelerate the convergence of the series.

V. THE WKB-BASED METHODS

The WKB-based methods are among the most popular approaches for calculating the complex frequencies of the quasinormal modes. This is because the calculations are relatively simple and in many cases yield quite accurate results. In this approach, we attempt to construct the approximate solutions of Eq. (5) using a modification of the WKB method. The asymptotic conditions near the event horizon and the conditions for the quasinormal modes lead to the equation relating frequencies and the behavior of the potential term near its maximum. Denoting $Q(x) = \omega^2 - V(x)$ and its consecutive derivatives calculated at by x_0 by Q_0, Q'_0, Q''_0, \dots , this equation can be written in the form

$$\frac{iQ_0}{\varepsilon \sqrt{2Q''_0}} - \sum_{k=2}^N \varepsilon^{k-1} \Lambda_k = n + \frac{1}{2}. \quad (39)$$

Here, each Λ_k is constructed from the derivatives of $Q(x)$ calculated at $x = x_0$, where the potential attains its maximum, and ε is the expansion parameter. Solving (39) with respect to ω one gets

$$\omega^2 = V(x_0) - i \left(n + \frac{1}{2} \right) \sqrt{2Q''_0} \varepsilon - i \sqrt{2Q''_0} \sum_{k=2}^N \varepsilon^k \Lambda_k. \quad (40)$$

The above formula can be used to perform a brief historical survey of the simple WKB-based methods. Retaining the first two terms in Eq. (40) results in the Schutz-Will approximation [21] (see also [22]). Furthermore, including the two next terms of the expansion, Λ_2 and Λ_3 , yields the well-known and widely used Iyer-Will method [23]. Finally, Konoplya calculated the terms Λ_k up to $N = 6$ and demonstrated that in many cases the results are close to the results of the exact numerical calculations [24]. In all these methods the Λ_k parameters are just summed and since $|\Lambda_k|$ grow fast with k one may ask if there is any point in increasing the number of retained Λ -terms. The answer to this doubt has been given in Ref. [12], in which all the terms up to $N = 13$ has been calculated analytically and since the summation of the Λ_k terms is generally a bad strategy in this regard, it has been proposed to construct the Padé approximants of Eq. (40). Specifically, in [12] it has been shown that for the well-documented complex frequencies of the quasinormal modes of the Schwarzschild and the Reissner-Nordström black holes, the Padé summation always gives the results that are in an excellent agreement with the exact numerical calculations. The methods presented in Ref. [12] has been subsequently extended in Ref. [13], where the analytical calculations has been carried out up to $N = 16$. Unfortunately, the analytic calculations of the higher-order terms are both time consuming and pose high demands on the computer resources, as the complexity of the Λ -terms rapidly increase with k . Since the dynamics of the calculations suggests that the most interesting are the higher orders of the WKB approximation it is natural that to make real progress and to make the calculations tractable one has to switch to numerics. The strategy would be, therefore, as follows. First, we calculate numerically all Λ_k up to required order and subsequently we accelerate the convergence of the sequence/series (or even make them convergent) using some standard methods, as for example, the Padé summation [12], the ϵ -Wynn acceleration [13], the Borel summation [25], and the Borel-Le Roy summation [20]. Finally, if possible, we compare the thus obtained results with the results constructed within the framework of other methods, as for example the Hill determinant method and its modifications [19] or the method of continued fraction [26].

In a very interesting development [27], Zaslavskii demonstrated that the problem of calculating complex frequencies of quasinormal modes can be reformulated as a bound-state problem. Similar considerations have been presented in Refs. [28, 29]. Specifically, Zaslavskii demonstrated that it is possible to reconstruct the main result of the Iyer and Will paper studying an anharmonic oscillator with corrections up to sixth-order. It should be noted that Zaslavskii's method may not be optimal for constructing the higher-order terms of the WKB approximation. Fortunately, in a very interesting paper [30] Sulejmanpasic and Ünsal extended to the arbitrary polynomial corrections

the classical results of Bender and Wu [31]. Their paper is accompanied with a powerful computer algebra package for fast and reliable calculations of the really high orders of the perturbation expansion. This package has been used in very accurate calculations of the complex frequencies of the quasinormal modes in Refs. [13, 20, 25, 32, 33].

VI. QUASINORMAL MODES

A. $(2+1)$ -dimensional analogue black hole

In determining the frequencies of the quasinormal modes of the $(2+1)$ -dimensional black holes, we restricted ourselves to the modes satisfying relations $1 \leq m \leq 6$ and $0 \leq n \leq m + 1$. The reason for this choice is twofold. First, the complex frequencies of the overtones (labeled here by n) of the low-lying fundamental modes (characterized by the azimuthal number m) are hard to be calculated precisely within the framework of the WKB-based method. Secondly, the low-lying modes are more likely to be detectable in laboratory settings, as the higher overtones are damped quickly and virtually play no role. Since our main task is to provide highly accurate results, that are correct to, say, 9 decimal places we decided to accept the result only if for a given m and n there is an agreement between the results obtained within the framework of at least two independent methods. In the vast majority of cases, we compared the frequencies obtained using the WKB method and the Hill determinant method. The continued fraction method has been used to check the correctness of the result to 9 decimal places. The computational strategy is as follows. First we calculate the frequencies of the quasinormal modes using either the higher-order WKB-*Padé* method or the higher-order WKB with the Wynn convergence acceleration algorithm. We deem the result acceptable if the frequencies remain unchanged to the prescribed accuracy as the order of the WKB increases. Typically, to ensure high accuracy for the overtones of the low-lying modes it is necessary to conduct the calculations up to some really big N and to retain as many digits in the decimal representation as needed. The final results were rounded to 64 decimal places. Subsequently, the frequencies thus calculated, when rounded to two decimal places, were used as the starting values in the Hill determinant method. For a given m and low n , the stable roots of the determinant equations, as functions of the dimension of the Hill submatrices, rapidly approach the exact frequency and one can easily obtain reasonable answers without additional effort. Unfortunately, the accuracy deteriorates as the overtone number increases, and one is forced to use the convergence acceleration techniques. Here, regardless of the type of the mode,

we used the Wynn algorithm to accelerate the convergence of the approximants. This approach makes it easier to automate the calculations.

Results of our calculations are tabulated in Tab. I. The first two columns specify the mode, N_{max} is the dimension of the maximal matrix, ω is the quasinormal mode rounded to 9 decimal places, and finally $\Delta\omega = \omega_{Hill} - \omega_{WKB}$, where ω_{Hill} and ω_{WKB} are the complex frequencies calculated within the framework of the Hill-determinant method and the WKB-Padé (or the WKB-Wynn method), respectively. For each mode, we solved the determinant equations

$$\det \mathcal{H}_k = 0 \tag{41}$$

for $6 \leq k \leq N_{max}$. Inspection of the table shows that the agreement between the results obtained within the framework of the Hill and the WKB method is, in most cases, truly remarkable. Except for the (1,1), (1,2), (2,3), and (3,4) modes, where the first element of the ordered pair is m and the second is n , the real and imaginary parts of $\Delta\omega$ are always smaller than 10^{-10} . To understand the origin of this (extremely small) discrepancy, let us analyze the behavior of the roots of the determinant equations for the (1,0), (1,1), and (1,2) modes. Let us start with the fundamental one. In this case (Fig. 1), convergence is rapid and the approximants are located along the spiral curve in the complex ω -plane. It is noteworthy that satisfactory results can be achieved even without convergence acceleration. On the other hand, the (1,1)-mode necessitates such an acceleration. Indeed, as can be seen in Fig. 2, the approximants lie along the spiral curve, but now for $6 \leq k \leq 850$ the convergence of ω_k is slower. (To enhance clarity, we included additional 250 points). Instead of further increasing N_{max} , we used the Wynn acceleration technique and, after some computations, we arrived at the result quoted in Tab. I and shown as a red dot in Fig. 2. The oscillatory character of the real and imaginary parts of ω_k is clearly visible in Figs. 3 and 4. Despite the fact that $\Delta\omega$ does not satisfy our accuracy criteria, we believe that the figures quoted in the table are correct, as they are also confirmed by the analogous calculations done using the continued fraction method. Finally, let us analyze the (1,2)-mode. The results of our calculations are shown in Fig. 5. We see that the convergence is really slow and to gain a better understanding of how successive ω_k are arranged on a complex plane, we connected the points corresponding to $k-1$ and k by line segments (Fig. 6). This explains why it is difficult to stabilize the result to the required precision, even after the applying the convergence acceleration algorithm. Now, inspection of Figs. 7 and 8 suggests that the exact value of ω should be close to the value displayed in the table. Once again the quoted ω has been compared with the analogous result calculated using the continued fraction method.

TABLE I. Quasinormal modes of the (2 + 1)-dimensional hydrodynamic black hole. m is the azimuthal number, n the overtone number, N_{max} is the maximal dimension of the Hill matrix, ω is the complex frequency calculated within the frameworks of the Hill determinant method and the continued fraction method and $\Delta\omega = \omega_{Hill} - \omega_{WKB}$. The high precision results of ω are rounded to 9 decimal places.

| m | n | N_{max} | ω | $\Delta\omega = \omega_{Hill} - \omega_{WKB}$ |
|-----|-----|-----------|--------------------------------|---|
| 1 | 0 | 300 | $0.4068326197 - 0.3412361181i$ | $-5.16 \times 10^{-14} + 1.29 \times 10^{-14}i$ |
| | 1 | 600 | $0.1974857187 - 1.2327917501i$ | $1.82 \times 10^{-6} - 4.5 \times 10^{-7}i$ |
| | 2 | 900 | $0.091780332 - 2.246129421i$ | $0.001055 - 0.000364i$ |
| 2 | 0 | 300 | $0.9527280877 - 0.3507394957i$ | $-4.17 \times 10^{-25} + 2.16 \times 10^{-25}i$ |
| | 1 | 600 | $0.7855826085 - 1.1248440726i$ | $-3.02 \times 10^{-21} - 6.4 \times 10^{-22}i$ |
| | 2 | 900 | $0.582309540 - 2.062341146i$ | $-1.37 \times 10^{-15} + 5.25 \times 10^{-15}i$ |
| | 3 | 1200 | $0.451386741 - 3.078412997i$ | $2.02 \times 10^{-11} + 1.56 \times 10^{-11}i$ |
| 3 | 0 | 100 | $1.468540697 - 0.352425533i$ | $-6.32 \times 10^{-19} - 4.49 \times 10^{-19}i$ |
| | 1 | 150 | $1.348492532 - 1.089552723i$ | $-1.42 \times 10^{-16} + 9.5 \times 10^{-17}i$ |
| | 2 | 200 | $1.145380889 - 1.922656549i$ | $4.51 \times 10^{-13} - 3.2 \times 10^{-14}i$ |
| | 3 | 250 | $0.942036373 - 2.870245548i$ | $-6.6 \times 10^{-11} + 4.44 \times 10^{-10}i$ |
| | 4 | 300 | $0.790721695 - 3.880709660i$ | $2.36 \times 10^{-8} - 3.34 \times 10^{-8}i$ |
| 4 | 0 | 100 | $1.976452714 - 0.352959421i$ | $3.43 \times 10^{-22} + 8.1 \times 10^{-23}i$ |
| | 1 | 150 | $1.884585741 - 1.076850329i$ | $-8.1 \times 10^{-22} - 3.63 \times 10^{-21}i$ |
| | 2 | 200 | $1.714004250 - 1.856157434i$ | $8.18 \times 10^{-19} - 8.32 \times 10^{-19}i$ |
| | 3 | 250 | $1.501085485 - 2.721858168i$ | $-9.65 \times 10^{-16} - 9.64 \times 10^{-16}i$ |
| | 4 | 300 | $1.297445508 - 3.672813327i$ | $5.04 \times 10^{-13} - 5.45 \times 10^{-13}i$ |
| | 5 | 350 | $1.133188616 - 4.676212409i$ | $-5.33 \times 10^{-11} + 5.99 \times 10^{-11}i$ |
| 5 | 0 | 100 | $2.481187498 - 0.353188338i$ | $-3.23 \times 10^{-25} + 3.85 \times 10^{-25}i$ |
| | 1 | 150 | $2.407098481 - 1.070993110i$ | $4.64 \times 10^{-25} + 8.1 \times 10^{-26}i$ |
| | 2 | 200 | $2.264886375 - 1.824027440i$ | $1.67 \times 10^{-23} - 1.6 \times 10^{-24}i$ |
| | 3 | 250 | $2.070976107 - 2.635991315i$ | $-3.77 \times 10^{-21} + 4.17 \times 10^{-21}i$ |
| | 4 | 300 | $1.855346091 - 3.521329941i$ | $9.0 \times 10^{-19} + 3.73 \times 10^{-18}i$ |
| | 5 | 350 | $1.651546102 - 4.473743454i$ | $-1.31 \times 10^{-15} + 5.9 \times 10^{-16}i$ |
| | 6 | 400 | $1.478994088 - 5.470943809i$ | $1.14 \times 10^{-13} - 1.17 \times 10^{-13}i$ |
| 6 | 0 | 100 | $2.984336621 - 0.353306306i$ | $-1.27 \times 10^{-27} - 1.31 \times 10^{-27}i$ |
| | 1 | 150 | $2.922346372 - 1.067823824i$ | $-7.4 \times 10^{-29} + 1.79 \times 10^{-28}i$ |
| | 2 | 200 | $2.801558110 - 1.806593575i$ | $4.53 \times 10^{-28} + 8.87 \times 10^{-28}i$ |
| | 3 | 250 | $2.630357486 - 2.586630216i$ | $-3.69 \times 10^{-26} + 5.97 \times 10^{-26}i$ |
| | 4 | 300 | $2.425007511 - 3.422706779i$ | $1.53 \times 10^{-23} - 1.61 \times 10^{-23}i$ |
| | 5 | 350 | $2.208931018 - 4.320895003i$ | $1.65 \times 10^{-21} - 1.028 \times 10^{-20}i$ |
| | 6 | 400 | $2.005051173 - 5.274064480i$ | $2.97 \times 10^{-18} - 3.7 \times 10^{-19}i$ |
| | 7 | 450 | $1.826891590 - 6.266212422i$ | $-2.49 \times 10^{-16} + 2.40 \times 10^{-16}i$ |

TABLE II. Fundamental modes of the $(2 + 1)$ and $(3 + 1)$ -dimensional hydrodynamic black hole calculated within the framework of the sixth-order WKB method without any convergence acceleration. Here, l is either the multipole number s or the azimuthal number m

| l | $l = m, \omega_{(2+1)}$ | $l = s, \omega_{(3+1)}$ |
|-----|-------------------------|-------------------------|
| 0 | | $0.05820 - 0.87431i$ |
| 1 | $0.42722 - 0.33011i$ | $1.09712 - 0.39365i$ |
| 2 | $0.95143 - 0.35304i$ | $1.41382 - 0.70152i$ |
| 3 | $1.46852 - 0.35248i$ | $2.12332 - 0.61734i$ |
| 4 | $1.97645 - 0.35296i$ | $2.75319 - 0.61870i$ |
| 5 | $2.48119 - 0.35319i$ | $3.38007 - 0.61989i$ |
| 6 | $2.98434 - 0.35331i$ | $4.00536 - 0.62027i$ |

Let us compare our results with the results that can be found in the literature. In Ref. [10], the authors calculated quasinormal frequencies of the fundamental modes ($n = 0$) for $1 \leq m \leq 4$ of the $(2+1)$ -dimensional hydrodynamic black hole using three simple WKB computational schemes. The schemes differ only in the number of terms retained in the right-hand-side of Eq. (40). The first one was developed by Schutz and Will in which one retains only two first terms, and their extensions based on the third-order ($N = 3$) and the sixth-order WKB approximation ($N = 6$). The thus obtained results were rounded to two decimal places. To make the comparison more accurate we have recalculated the fundamental modes for $1 \leq m \leq 6$, using the sixth-order WKB method independently and retained more decimal places. The results of our calculations are presented in Tab. II. First, it should be noted that our result for the mode $(2,0)$ differs substantially from the analogous frequency calculated in Ref. [10] and since our result has been confirmed by the two algorithmically different calculations we believe that our result is correct. Now, we can compare the results presented in Tab. II with the more accurate results displayed in Tab. I. As expected, larger discrepancies between our results and those presented in Ref. [10] are observed in the lower modes and the agreement improves progressively as the azimuthal number, m , increases. This behavior can be attributed to the increase of the real part of the complex frequencies of the fundamental modes along with the relatively weak change in their imaginary parts. Typically, WKB-based methods for computing quasinormal modes (without application of any additional techniques, as, for example, convergence acceleration) are accurate for the frequencies satisfying $|\Re(\omega)| > |\Im(\omega)|$ and become less reliable when $|\Im(\omega)|$ increases.

Specifically, for mode $(1,0)$ one has relative error 5% and 3.3% for the real and the imaginary

parts, respectively, and the accuracy increases with m . We have not attempted to make a similar comparison for the overtones, but on general grounds, we expect that the accuracy of the sixth-order WKB rapidly deteriorates with the increase of n . Indeed, for a given m and increasing overtone number $\Re(\omega)$ decreases and $|\Im(\omega)|$ increases, leading to a deterioration in the quality of the approximation.

Since the master equation of the $(2 + 1)$ -dimensional analogue black hole is identical to the equation describing the electromagnetic vector perturbation of the five-dimensional Schwarzschild-Tangherlini black hole for $l \geq 2$, it is possible to extract valuable information from the calculations that have been carried out earlier. Indeed, it can easily be shown that the results presented here are consistent with those reported in Ref. [34]. Moreover, a comparison of the complex frequencies listed in Tabs. VII - IX of Ref. [20] and Tab. I of the present paper shows perfect agreement. It should be emphasized, however, that the results presented here are a significant extension of the previous ones.

Finally, we make a few observations regarding the general behavior of the modes. Let us start with the fundamental frequencies ($n = 0$). Inspection of Tab. I shows that their real part increases whereas the imaginary part very slowly decreases with m . For the first overtones ($n = 1$) the situation is different: both the real part and the imaginary part increases and this trend also persists for higher overtones. On the other hand, for a given azimuthal number m the real and imaginary part of the complex frequencies decreases.

B. $(3 + 1)$ -dimensional analogue black hole

Let us consider the $(3 + 1)$ -dimensional hydrodynamic black hole. Unlike the previous case of the $(2 + 1)$ -dimensional black hole, there are no simple relations between l and s in Eqs. (14) and (5) with (9), respectively. Since the application of the continued fraction method require, depending on the choice of the recurrence relation, either five or three consecutive Gauss eliminations, we will not use this technique in this case. Instead, we will apply the Hill determinant method for both recurrences (23) and (26), and compare the thus obtained results with the calculations carried out within the framework of the higher-order WKB method with the convergence acceleration. Once again, we accept the thus obtained result only if at least two independent calculations agree to the required precision and the calculations based on two different recursive schemes are considered as independent.

The results of the calculations are presented in Tab. III. Comparing the performance of the

methods we observe that the WKB is slightly less accurate, particularly for the lowest fundamental mode. However, for the remaining modes the agreement is really truly remarkable. On the other hand, since for the $s = 0$ and $n = 0$ mode both recurrences give the same result to the assumed accuracy, we believe that the quoted figures are correct. Now, we can compare our results with the results discussed in Ref. [10]. Since the authors employed simple first, third, and sixth-order WKB methods, the agreement of the first two fundamental modes is poor. In particular, we do not confirm statement that for the fundamental $s = 0$ and $s = 1$ modes the lowest WKB approximation gives the most reliable results. We have recalculated the sixth-order WKB results using our codes, extending the calculations to $s = 6$ and retained more digits. Inspection of the Tabs. II and III shows, that for $s \geq 1$ it is the sixth-order WKB that agrees the best with our results. On the other hand however, for the $(s = 0, n = 0)$ mode, all the three simple approximations yield very poor results. Since both the real and the modulus of the imaginary part of ω rapidly grow in magnitude as the order of the WKB increases, our conclusion is that it is not possible to obtain sensible results for the $(s = 0, n = 0)$ mode without some modification of the method.

Inspection of Tab. III shows that for the fundamental quasinormal modes both the real part of its frequency increases and the imaginary part slowly decreases as the s number increases (an exception here is the $(0, 0)$ mode). It seems that this weak dependence of $\Im(\omega)$ on s is typical for both acoustic black holes. For the lowest overtones ($n = 1$) both real and imaginary part of ω increase. On the other hand, for a given s both the real part and the imaginary part of the frequency decrease.

A typical migration of the consecutive approximations to the frequency of the quasinormal mode $s = 2$ and $n = 2$ is shown in Figs. 9 and 10. Each point on the complex plane is a particular solution of the Hill determinant equations calculated with the same initial condition. The red point represents the limit $\omega = 0.422044365 - 4.200890173i$. For a better visibility we have connected k and $k - 1$ points by line segments, where k is the dimension of the Hill matrix. Since the solutions of the determinant equation lie on the spiral-like curve the real and the imaginary parts of ω reveal the oscillatory character. This behavior resembles the behavior of the quasinormal modes of $(2 + 1)$ -dimensional analogue black holes.

VII. FINAL REMARKS

In this paper we have calculated the complex frequencies of the quasinormal modes, ω , of the two models of the analogue black holes: the $(2 + 1)$ -dimensional draining bathtub black hole and the

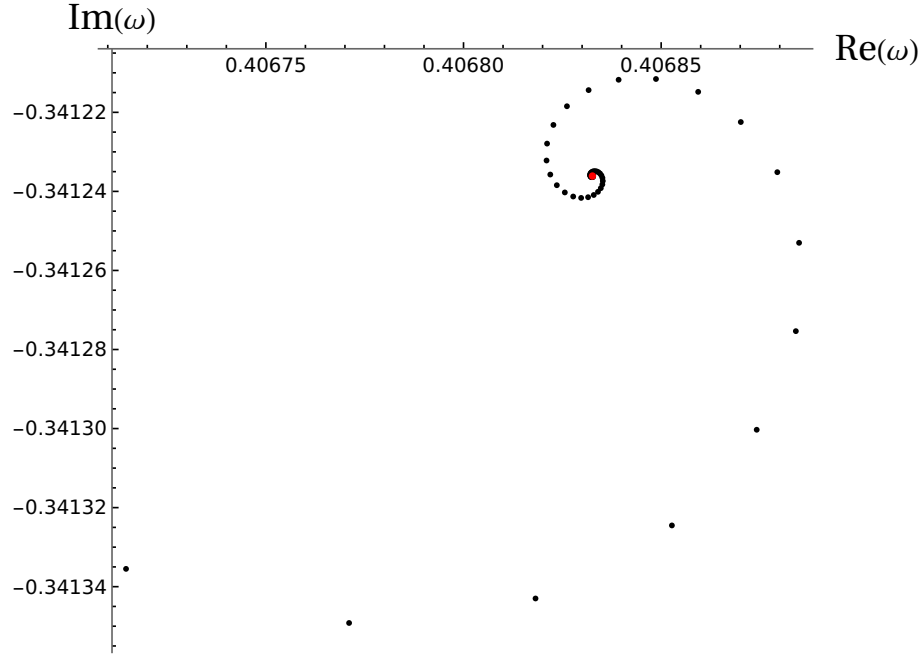


FIG. 1. The $(2+1)$ -dimensional hydrodynamic black hole. Migration of the approximants of the complex frequency of the $m = 1$, $n = 0$ mode on the complex plane. The red dot represents the limiting value calculated using the Wynn acceleration algorithm.

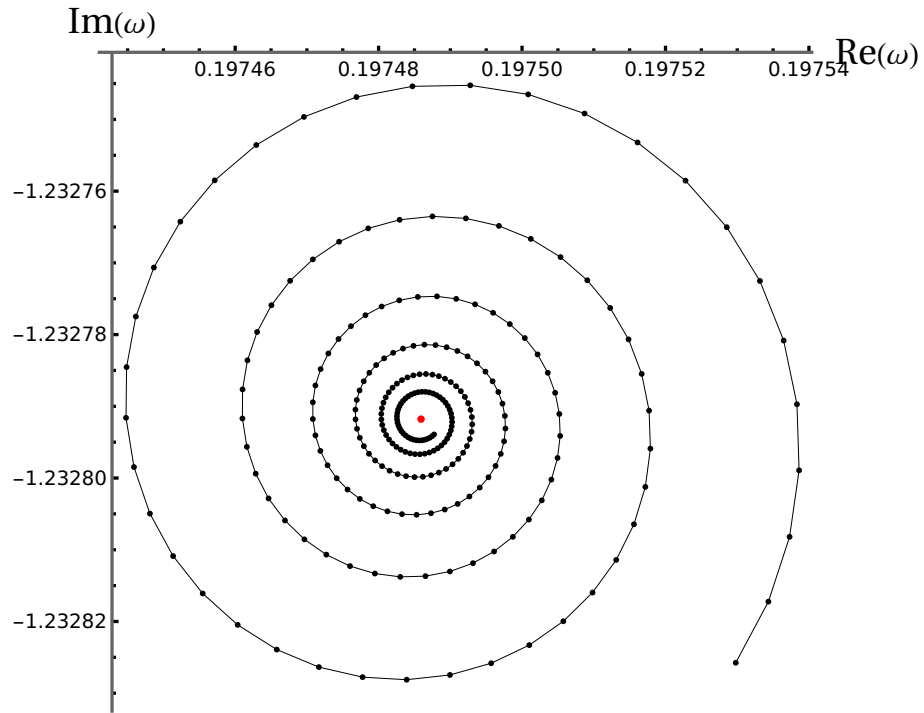


FIG. 2. The $(2+1)$ -dimensional hydrodynamic black hole. Migration of the approximants of the complex frequency of the $m = 1$, $n = 1$ mode on the complex plane. The red dot represents the limiting value calculated using the Wynn acceleration algorithm.

TABLE III. Quasinormal modes of the $(3 + 1)$ -dimensional hydrodynamic black hole. s is the multipole number, n is the overtone number, N_{max} is the maximal dimension of the Hill matrix, ω is the complex frequency calculated within the frameworks of the Hill determinant method and $\Delta\omega = \omega_{Hill} - \omega_{WKB}$. The high precision results of ω are rounded to 9 decimal places.

| s | n | N_{max} | ω | $\Delta\omega = \omega_{Hill} - \omega_{WKB}$ |
|-----|-----|-----------|------------------------------|---|
| 0 | 0 | 300 | $0.072813815 - 0.619901186i$ | $4.09 \times 10^{-5} - 2.53 \times 10^{-5}i$ |
| 1 | 0 | 200 | $0.816775035 - 0.611054595i$ | $-1.16 \times 10^{-15} - 2.51 \times 10^{-15}i$ |
| 2 | 0 | 250 | $1.479691724 - 0.617355106i$ | $2.65 \times 10^{-22} + 5.06 \times 10^{-22}i$ |
| | 1 | 300 | $0.919814109 - 2.070617645i$ | $1.91 \times 10^{-9} + 2.45 \times 10^{-10}i$ |
| 3 | 0 | 200 | $2.120221930 - 0.619367816i$ | $-7.12 \times 10^{-25} + 5.18 \times 10^{-25}i$ |
| | 1 | 250 | $1.712558987 - 1.947807598i$ | $4.46 \times 10^{-18} + 1.67 \times 10^{-19}i$ |
| | 2 | 300 | $0.984422651 - 3.769874878i$ | $-7.03 \times 10^{-9} + 1.59 \times 10^{-8}i$ |
| 4 | 0 | 150 | $2.752103594 - 0.620056709i$ | $1.04 \times 10^{-23} + 9.03 \times 10^{-24}i$ |
| | 1 | 200 | $2.437907970 - 1.909000239i$ | $-2.50 \times 10^{-21} - 4.30 \times 10^{-21}i$ |
| | 2 | 250 | $1.775391582 - 3.433842488i$ | $-8.05 \times 10^{-14} + 1.86 \times 10^{-14}i$ |
| | 3 | 300 | $1.109803434 - 5.521445321i$ | $6.01 \times 10^{-8} - 2.68 \times 10^{-8}i$ |
| 5 | 0 | 100 | $3.379842300 - 0.620312172i$ | $1.75 \times 10^{-21} - 1.74 \times 10^{-21}i$ |
| | 1 | 150 | $3.124541370 - 1.891903509i$ | $-3.15 \times 10^{-20} - 5.09 \times 10^{-20}i$ |
| | 2 | 200 | $2.585373209 - 3.290233538i$ | $-8.95 \times 10^{-18} + 2.95 \times 10^{-18}i$ |
| | 3 | 250 | $1.806285519 - 5.064977404i$ | $4.61 \times 10^{-12} + 5.12 \times 10^{-12}i$ |
| | 4 | 300 | $1.259981716 - 7.272525138i$ | $5.36 \times 10^{-8} + 6.43 \times 10^{-8}i$ |

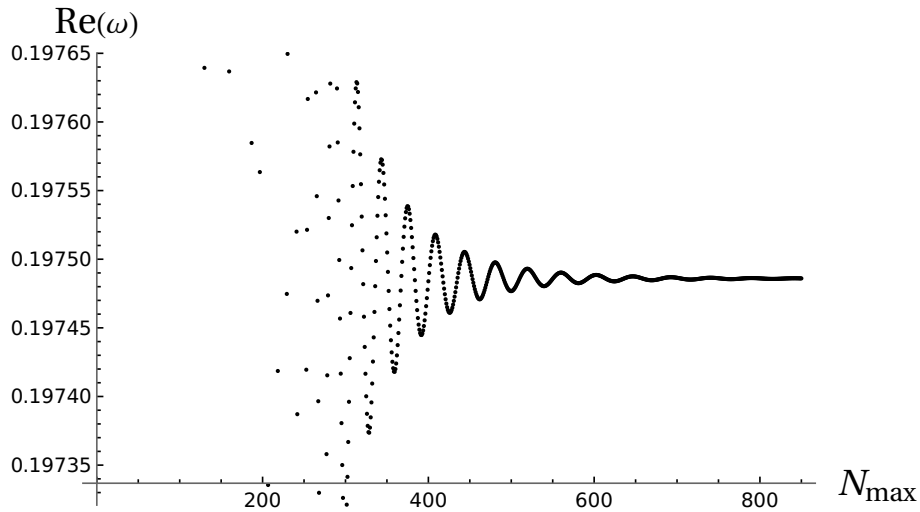


FIG. 3. The $(2 + 1)$ -dimensional hydrodynamic black hole. The real part of the quasinormal frequency of the $m = 1, n = 1$ perturbation as a function of the dimension of the Hill matrix.

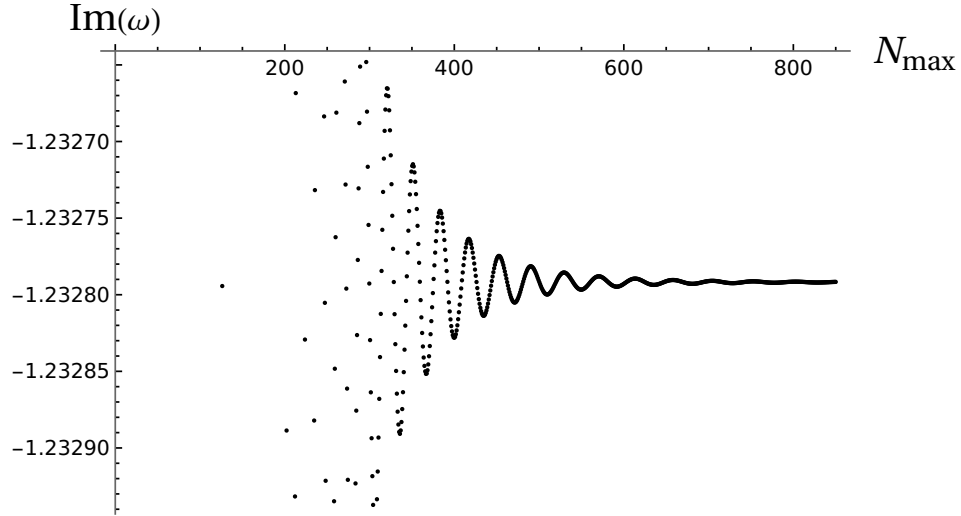


FIG. 4. The $(2+1)$ -dimensional hydrodynamic black hole. The imaginary part of the quasinormal frequency of the $m = 1$, $n = 1$ perturbation as a function of the dimension of the Hill matrix.

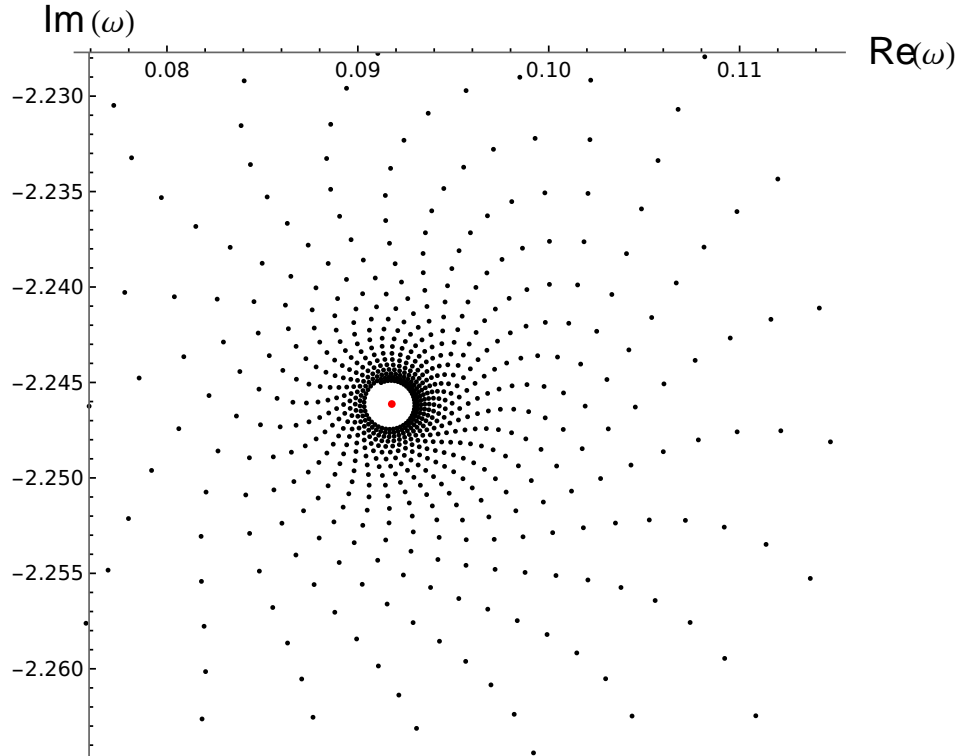


FIG. 5. The $(2+1)$ -dimensional hydrodynamic black hole. Migration of the approximants of the complex frequency of the $m = 1$, $n = 2$ mode on the complex plane. The red dot represents the limiting value calculated using the Wynn acceleration algorithm.

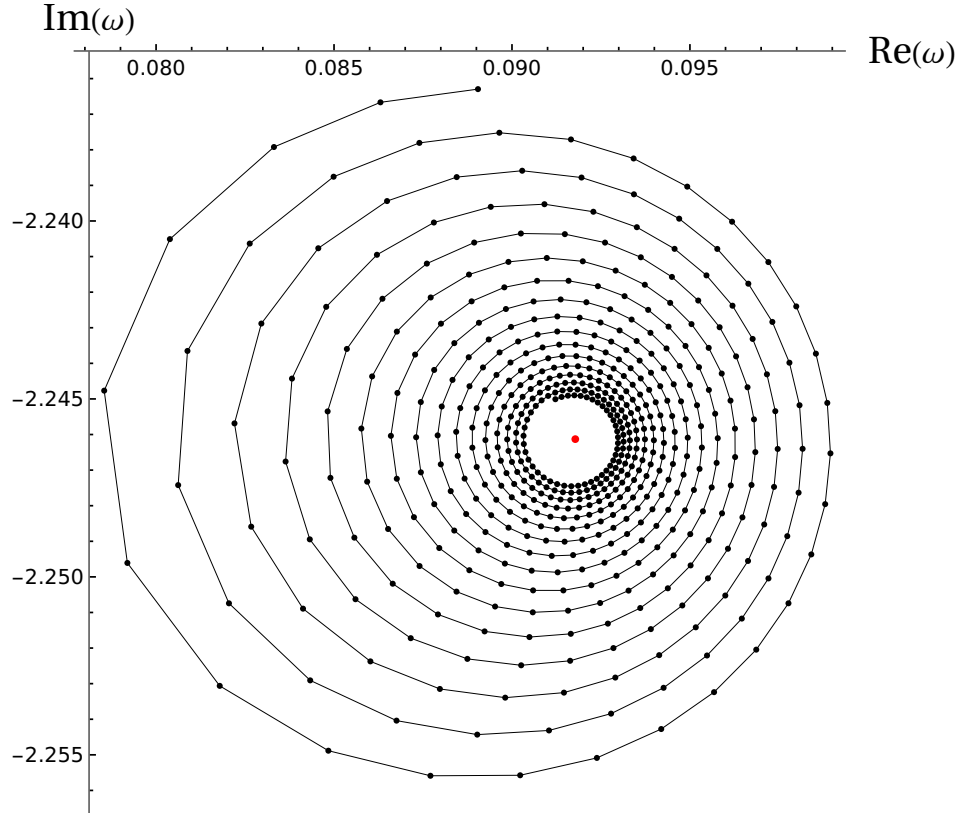


FIG. 6. The $(2 + 1)$ -dimensional hydrodynamic black hole. Migration of the approximants of the complex frequency of the $m = 1$, $n = 2$ mode on the complex plane. The red dot represents the limiting value calculated using the Wynn acceleration algorithm. The N -th approximants in connected by a line segment with the $N + 1$.

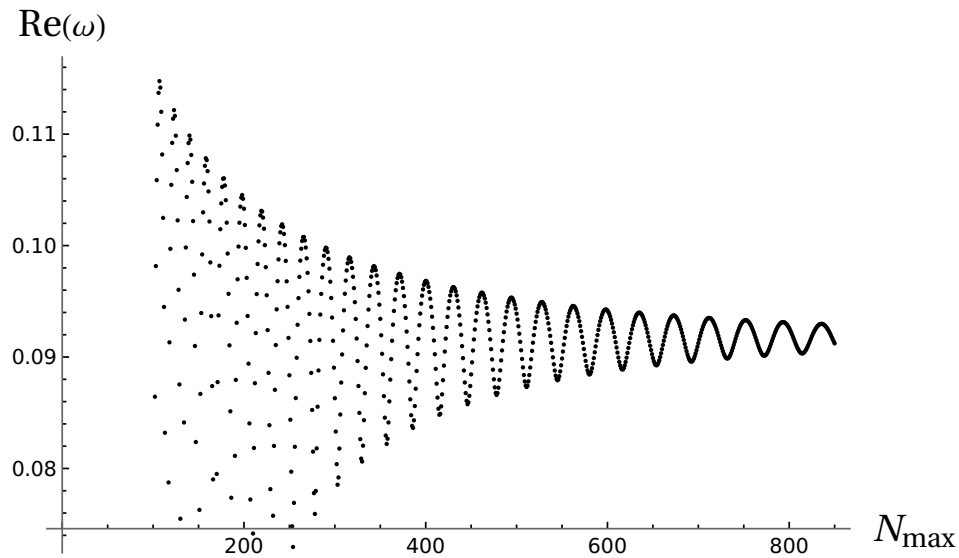


FIG. 7. The $(2 + 1)$ -dimensional hydrodynamic black hole. The real part of the quasinormal frequency of the $m = 1$, $n = 2$ perturbation as a function of the dimension of the Hill matrix..

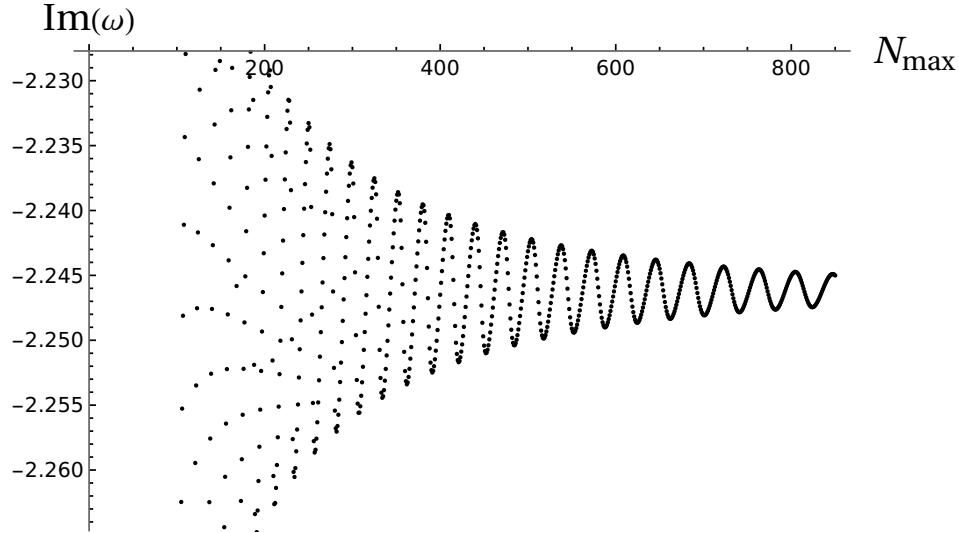


FIG. 8. The $(2+1)$ -dimensional hydrodynamic black hole. The imaginary part of the quasinormal frequency of the $m = 1, n = 2$ perturbation as a function of the dimension of the Hill matrix..

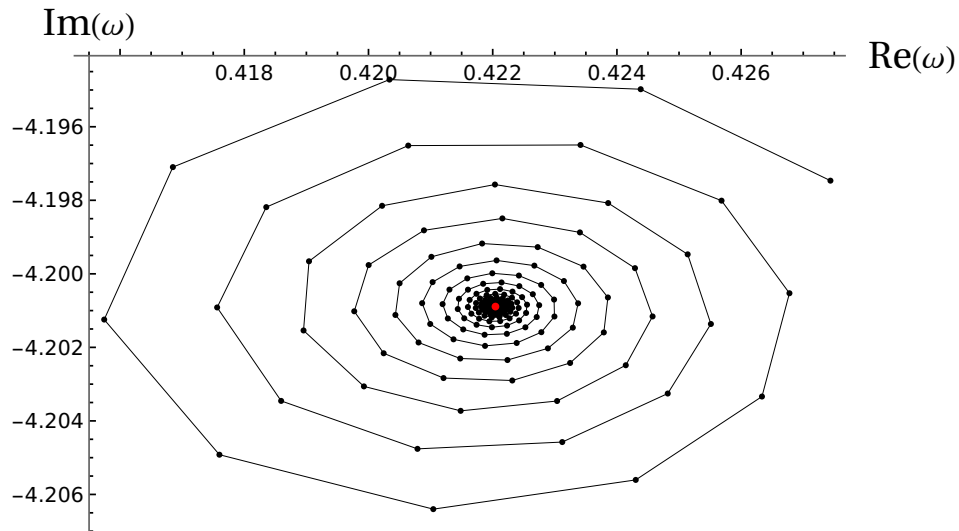


FIG. 9. The $(3+1)$ -dimensional hydrodynamic black hole. Migration of the approximants of the complex frequency of the $s = 2, n = 2$ mode on the complex plane. The red dot represents the limiting value calculated using the Wynn acceleration algorithm. The N -th approximants in connected by a line segment with the $N + 1$.

$(3+1)$ -dimensional canonical acoustic black hole. The perturbations satisfy the Schrödinger-type differential equations and the complexity of the potential terms effectively preclude construction of the exact solutions. Our calculations were performed within the frameworks of the three major techniques: the Hill-determinant method with the convergence acceleration, the continued fraction method also with the convergence acceleration, and the higher-order WKB-Padé method (or its

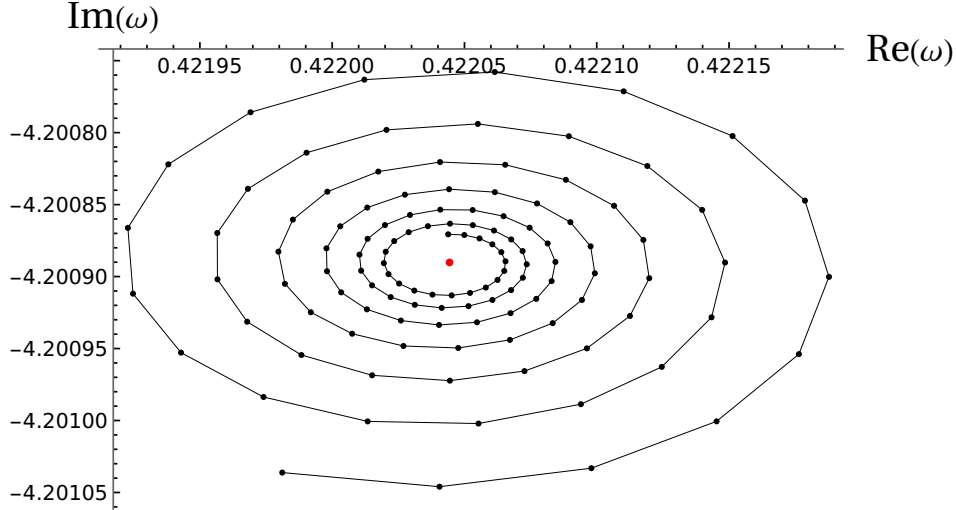


FIG. 10. The central region of Fig. 9. The red dot represents the limiting value calculated using the Wynn acceleration algorithm.

modifications). Each of the methods have its strong and weak points, and one of our principal tasks was comparison their the effectiveness and performance. The other two tasks were: calculation of the highly accurate ω , say to 9 decimal places, and extending (and sometimes correcting) the results found in the literature. Moreover, knowledge of the highly accurate and well-documented quasinormal modes may play a crucial role in the development of new computational methods and techniques.

The signal from such hydrodynamic systems will certainly not be pure. On the contrary, the signal from the man-made acoustic black hole will be contaminated by other frequencies related to the way the black hole would be excited, characteristics of the setup, and many other factors. It is therefore crucial to have solid theoretical predictions at one's disposal.

Now, we provide a brief characterization of each method in the context of the obtained results. Our calculations indicate that all of them work very well. There are however some differences in their performance. Undoubtedly, the strength of the WKB-Padé method lies in its black-box nature. Once the potential $V(r)$ for a given l and the overtone number is known, the application of the simple algorithm yields reasonable (in the most cases) results. The limitations are typical for any method based on the WKB approximation: the results deteriorate for higher overtones. It remains an open question whether this can be circumvented by increasing the number of the Λ_k terms left in Eq. (40). We know that increasing the order of the WKB approximation results in rapid increase of the absolute values of the real and imaginary parts of the quasinormal frequency. So the above question is, in fact, a question regarding the effectiveness of the Padé summation or other

techniques for convergence acceleration.

On the other hand, the Hill-determinant method is slightly more complicated. It requires knowledge of the analytical structure of the radial equation and the construction of appropriate recurrence relations for the numerical coefficients of the series expansion of its solutions. As the approximate quasinormal modes are a subset of the set of all solutions of the determinant equation, it is necessary to define some criteria for selecting solutions that are of interest to us. Our strategy is as follows: First, we calculate interesting mode using some low-cost method, and subsequently use it as a starting point for constructing the solution of the determinant equations for increasing dimension of the Hill matrices. The thus determined solutions migrate on a complex plane and in order to calculate the final result we accelerate convergence using the Wynn algorithm. This procedure yields very accurate results.

The third approach that has been used in this paper (but only in the case of the $(2 + 1)$ -dimensional acoustic black hole) is the continued fractions method. It relies on the same recurrence relations as the Hill-determinant method and utilizes the deep relationship between three-term recursion and the continued fractions. Since the recurrences considered in this paper involve more terms than three, it is necessary to apply successive Gauss eliminations. Now, the evaluation of the continued fractions leads to the rational functions, which can be solved numerically for the characteristic frequencies of the quasinormal modes. Once again, to accelerate convergence of the results we used the Wynn algorithm. In this form, the continued fractions method is comparable in effectiveness to the Hill-determinant method. However, there are two important differences. In the Hill determinant method, there is no need for transforming the matrix to the tridiagonal form, which considerably simplifies calculations. On the other hand, the continued fraction method has a mechanism for evaluating the tail terms, a feature that improves quality of the approximation.

Our calculations demonstrate that all three methods work very-well and indicate that we have achieved assumed accuracy. Specifically, in the $(2+1)$ -dimensional case both the continued fraction method and the Hill determinant method always give the same results to (at least) 9 decimal places. The performance of the higher-order WKB-Padé method is also very good, as can be seen in the tables. In the $(3 + 1)$ -case, instead of employing the continued fraction method we used two recurrence relations: the eight-term and the six-term ones. Once again, we have excellent agreement in the results obtained in each of these approaches. It should be emphasized that the convergence acceleration is an indispensable tool, especially for the overtones and the methods presented here can easily be adapted to other types of black holes.

ACKNOWLEDGMENTS

JM was partially supported by Grant No. 2022/45/B/ST2/00013 of the National Science Center, Poland.

Appendix: Recurrences

The recurrence relations (20), (23), and (26) have been calculated for the analogue black holes. They are, respectively, the special cases of the recurrence relations of the five-dimensional and the seven-dimensional Schwarzschild-Tangherlini black holes. Here, we collect the coefficients of the general recurrence equation

$$a_{k+1} \alpha_k + a_k \beta_k + a_{k-1} \gamma_k + a_{k-2} \delta_k + a_{k-3} \kappa_k + a_{k-4} \lambda_k + a_{k-5} \mu_k + a_{k-6} \nu_k = 0. \quad (\text{A.1})$$

In the formulae below, $L = l(l + D - 3)$, D is the dimension of the Schwarzschild-Tangherlini black hole, $T = 1 - j^2$, where j is the type of perturbation given in (15), and finally $a_k = 0$ for $k \leq -1$. The coefficients of the four-term recurrence ($\kappa_k = \lambda_k = \mu_k = \nu_k = 0$) are given by

$$\begin{aligned} \alpha_k &= -2(k+1)(k-2\rho+1), \\ \beta_k &= 5k^2 + k(5-16\rho) + L + 16\rho^2 - 8\rho + \frac{9T}{4} + \frac{3}{4}, \\ \gamma_k &= -4k^2 + 8k\rho - \frac{9T}{2} + 4, \\ \delta_k &= k^2 - k + \frac{9T}{4} - 2. \end{aligned} \quad (\text{A.2})$$

In the case of the seven-dimensional Schwarzschild-Tangherlini black hole one has either the six-term recurrence relation with ($\mu_k = \nu_k = 0$)

$$\begin{aligned} \alpha_k &= -4(k+1)(k-\rho+1), \\ \beta_k &= 14k^2 + k(14-24\rho) + L + 12\rho^2 - 12\rho + \frac{25}{4}T + \frac{15}{4}, \\ \gamma_k &= -20k^2 + 28k\rho - 8\rho^2 - 25T + 20, \\ \delta_k &= 15k^2 - k(16\rho+15) + 4\rho^2 + 8\rho + \frac{75}{2}T - 30, \\ \kappa_k &= -6k^2 + 4k(\rho+3) - 4\rho - 25T + 18 \\ \lambda_k &= k^2 - 3k + \frac{25}{4}T - 4. \end{aligned} \quad (\text{A.3})$$

or the eight-term recurrence

$$\begin{aligned}
\alpha_k &= -8(k+1)(k-\rho+1), \\
\beta_k &= 36k^2 - 64k\rho + 28k + 2L + 28\rho^2 - 28\rho + \frac{25}{2}T + \frac{15}{2}, \\
\gamma_k &= -72k^2 + 4k(34\rho+9) - 2L - 66\rho^2 - 32\rho - \frac{125}{2}T + \frac{57}{2}, \\
\delta_k &= 84k^2 - 152k(\rho+1) + L + 69\rho^2 + 142\rho + \frac{525}{4}T - \frac{113}{4}, \\
\kappa_k &= -2(31k^2 - k(49\rho+97) + 18\rho^2 + 80\rho + 75T + 12), \\
\lambda_k &= 29k^2 - 3k(12\rho+43) + 9\rho^2 + 84\rho + 100T + 52, \\
\mu_k &= -8k^2 + 6k\rho + 46k - 18\rho - \frac{75}{2}T - 30, \\
\nu_k &= k^2 - 7k + \frac{25}{4}T + 6.
\end{aligned} \tag{A.4}$$

It should be noted that in general we do not restrict j to the values given in (15).

-
- [1] W. G. Unruh, Phys. Rev. Lett. **46**, 1351 (1981).
 - [2] C. Barcelo, S. Liberati, and M. Visser, Living reviews in relativity **14**, 1 (2011).
 - [3] T. Torres, S. Patrick, M. Richartz, and S. Weinfurtnner, Phys. Rev. Lett. **125**, 011301 (2020).
 - [4] S. R. Dolan, L. A. Oliveira, and L. C. B. Crispino, Phys. Rev. D **85**, 044031 (2012).
 - [5] M. Visser, Classical and Quantum Gravity **15**, 1767 (1998).
 - [6] K. D. Kokkotas and B. G. Schmidt, Living Rev. Rel. **2**, 2 (1999).
 - [7] E. Berti, V. Cardoso, and A. O. Starinets, Class. Quant. Grav. **26**, 163001 (2009).
 - [8] R. A. Konoplya and A. Zhidenko, Rev. Mod. Phys. **83**, 793 (2011).
 - [9] H.-P. Nollert, Class. Quant. Grav. **16**, R159 (1999).
 - [10] E. Berti, V. Cardoso, and J. P. Lemos, Phys. Rev. D **70**, 124006 (2004).
 - [11] V. Cardoso, J. P. Lemos, and S. Yoshida, Phys. Rev. D **70**, 124032 (2004).
 - [12] J. Matyjasek and M. Opala, Phys. Rev. D **96**, 024011 (2017).
 - [13] J. Matyjasek and M. Telecka, Phys. Rev. D **100**, 124006 (2019).
 - [14] H. T. Cho, A. S. Cornell, J. Doukas, T. R. Huang, and W. Naylor, Adv. Math. Phys. **2012**, 281705 (2012).
 - [15] A. Jansen, Eur. Phys. J. Plus **132**, 546 (2017).
 - [16] G. Gibbons and S. A. Hartnoll, Phys. Rev. D **66**, 064024 (2002).
 - [17] A. Ishibashi and H. Kodama, Prog. Theor. Phys. **110**, 901 (2003).
 - [18] H. Kodama and A. Ishibashi, Prog. Theor. Phys. **111**, 29 (2004).
 - [19] B. Majumdar and N. Panchapakesan, Phys. Rev. D **40**, 2568 (1989).
 - [20] J. Matyjasek, Phys. Rev. D **104**, 084066 (2021).
 - [21] B. F. Schutz and C. M. Will, Astrophys. J. **291**, L33 (1985).

- [22] B. Mashhoon, in *Third Marcel Grossmann Meeting on General Relativity* (North-Holland, 1982).
- [23] S. Iyer and C. M. Will, *Phys. Rev. D* **35**, 3621 (1987).
- [24] R. A. Konoplya, *Phys. Rev. D* **68**, 024018 (2003).
- [25] Y. Hatsuda, *Phys. Rev. D* **101**, 024008 (2020).
- [26] E. W. Leaver, *Proc. Roy. Soc. Lond. A* **402**, 285 (1985).
- [27] O. B. Zaslavskii, *Phys. Rev. D* **43**, 605 (1991).
- [28] H. Blome and B. Mashhoon, *Physics Letters A* **100** (1984).
- [29] V. Ferrari and B. Mashhoon, *Phys. Rev. Lett.* **52**, 1361 (1984).
- [30] T. Sulejmanpasic and M. Ünsal, *Comput. Phys. Commun.* **228**, 273 (2018).
- [31] C. M. Bender and T. T. Wu, *Phys. Rev. D* **7**, 1620 (1973).
- [32] J. Matyjasek, *Phys. Rev. D* **102**, 124046 (2020).
- [33] J. Matyjasek and M. Telecka, *Phys. Rev. D* **107**, 064058 (2023).
- [34] V. Cardoso, J. P. S. Lemos, and S. Yoshida, *Phys. Rev. D* **69**, 044004 (2004).